Hindawi
Mathematical Problems in Engineering
Volume 2022, Article ID 3755574, 13 pages
https://doi.org/10.1155/2022/3755574

*Research Article*

# Optimization of Multisource Dynamic Model in TBO

**Xia Li, Hao Yan, and Yichi Zhang**

*College of Air Traffic Management, Civil Aviation Flight University of China, Deyang, Sichuan 618307, China*

Correspondence should be addressed to Hao Yan; yanhao19980907@163.com

Received 13 December 2021; Revised 5 January 2022; Accepted 12 January 2022; Published 4 February 2022

Academic Editor: Chengwei Fei



When extracting flight data from airport terminal area, there are matters such as large volume, unclear features, and similar trend in time series. In order to deal with the related issues and to optimize the description, by combining with the TBO (Trajectory-Based Operation), an application proposed by the ICAO (International Civil Aviation Organization) in ASBU (Aviation System Block Upgrade), using multisource dynamic model to establish 4DDW (4D dynamic warping) algorithm, the multisource modeling integrated with evaluation system is proposed to realize the flight path optimization with time series characteristics and accord with the interval concept. The calculation results show that 4DDW can obtain the optimal solution for multiprofile calculation of TBO by comparing the composite trajectory deviation values and time dimension planning using the buffer and threshold values recommended by ICAO in airspace planning and flight procedure design. The results meet the requirements of high accuracy and convergence features of spatial waypoints and can improve the airport operation standards and terminal area capacity.

## 1. Introduction

At present, the demand of air transports increases rapidly and stably. Even under the influence of extremely adverse events worldwide, the traffic volume of air transport briefly decreased but recovered quickly and continued to grow, indicating that the demand for air transport is still strong. For example, the industry was affected by the 911 event in the United States in 2001 and the global financial crisis in 2008, as well as the global COVID-19 pandemic in 2020 [1]. Thus, the air transportation industry can be suitable for long-term development, and the future air transportation will undergo a period of rapid global scientific and information technology development [2]. To fully implement the digital, intelligent, and high-quality development of air transportation, new requirements are put forward [3].

The high-quality developments of air transport are affected by many factors, from the perspective of airspace planning, laying out flight phases and flight procedures in the terminal area reasonably, setting up control sectors scientifically, utilizing three-dimensional space waypoints efficiently, etc., which are effective measures to ensure flight safety, promoting airspace capacity, and optimizing the setting of airspace and flight level. In order to further improve the normal implementation of operational measures, the accurate, efficient, and fast aeronautical information is required to enable the intelligent operation of flight missions [4]. To this end, the ICAO proposed the concept of ASBU (Aviation System Block Upgrades) [5], while the United States advanced the NEXTGEN [6] and Europe came up with the 'Single European Sky Project' [7]. The composition of a new generation of aeronautical information structure has been promoted by a series of theoretical innovations and technological breakthroughs. Among them, the 4D flight path planning and management researches are the most popular among the above concepts [8].

The essence of 4D flight path planning and management research is to collect, analyze, and evaluate aeronautical information comprehensively, and to deduce forward-looking operational conditions [9]. The digitalization requirements of this technology are reflected in the establishments of data collections, processing, and quality control standards [10], and the intellectualization is presented not only by the advance acquisitions and characterization analyses of various operational parameters [11], but also in the application of aeronautical information conclusions such as

the automatic generation of predictable spatial planning schemes [12]. Among those conclusions, the expected arrival and departure time of the flight, the spatial relative position relationship in each flight phase [13], the external disturbances that will be faced, and the expected fuel consumption [14], even the adaptability of the aircraft performance to the operating environment in each phase, are all important factors that affect whether a flight mission can be carried out as planned, and also as the basic parameters of flight path planning and management [15].

Early research on 4D trajectory prediction mainly focused on deviation calculation and accuracy of spatial location points. Liu et al. described and classified various basic models and algorithms of 4D flight path planning [16]. On that basis, Wang et al. proposed an approach procedure design method for airport terminal area, based on control applicability analysis, and applied the Euclidean distance model to deal with the flight trajectory prediction problems [17]. Ma et al. introduced a dynamic time warping method by the prediction of horizontal trajectory [18]. On this basis, Ding et al. added the twin support vector regression theory and further established a coordinate system-oriented flight conflict warning indicator [19] and completed the automatic generation of track through model building and calculation, providing a reference for the precise management of approach time [20]. Feng et al. referred to a point merge-based technology of 4D flight path planning method, which can greatly improve flight efficiency in the terminal area [21]. The above researches defined a preliminary concept for flight path planning, and those research conclusions, algorithms, and models have also established a calculation model for dealing with the overall trajectory design of aircraft, which has a certain reference. However, the evaluation system is too complicated and the flight details such as vertical profile, velocity profile, and altitude profile in each phase are not carried out, and the complete generalization of aeronautical information is not realized [22]. In addition, without considering the differences in issues such as flight safety, data complexity, and airspace width [23], it is impossible to complete refined and quantifiable assessment and prediction in air transportation [24]. In short, there is still much room for in-depth research [25].

## 2. Problem Description

4D flight path planning is based on the traditional three-dimensional flight path of aircraft, namely, longitude, latitude, and altitude, and integrates the time dimension to launch the flight path planning [26]. Since it is based on digitalization of aeronautical information, it is necessary to be organized and clustered for the horizontal tracks, and the model design is carried out by using vertical profiles, velocity profiles, and altitude profiles, so as to enable accurate prediction of spatial position points [27–29]. In addition, due to the problems of spatial overlap and flight trend similarity in historical radar trajectories, and lack of reliable mathematical descriptions for problems such as spatial path identification and flight environment measurements, as well as the insufficient data types and features of evaluation process [30], the 4D flight path calculation results are hardly supportive for actual flights [31].

In order to solve the above problems, hierarchical clustering method is proposed to improve the dynamic spatial warping algorithm. The evaluation model is designed for the vertical profile, velocity profile, and altitude profile of each flight phase, to enable multidata generalization and feature analysis, to take the flight parameters and spatial position data of each waypoint in the arrival segment as the collection object, to obtain the deviation value through each profile evaluation model, to form 4D flight path optimization data by combining with ICAO setting of BV (buffer value) in flight safety evaluation, and to realize spatial position point prediction and path generation based on 4D flight path planning [32].

## 3. Model Building

Because the historical flight trajectories, navigation, and other data have the features of large volume, low data quality and reliability, and different presentations [33], the flight trajectory has the need for convergence processing and deviation correction standardizing its mathematical description, due to the factors of navigation accuracy and operating environment. Preprocessing according to data classification, applying HCDT (hierarchical clustering dynamic time warping), DSW (dynamic spatial warping), and HPO (height profile optimization) algorithm are carried out to analyze and process data under each flight phase respectively. The conclusions of flight trajectory and time dimension are obtained by simulation experiments. With comparing $t_{PTA}$ and $t_{ETA}$ thresholds, the flight path prediction based on the 4DDW (4D dynamic warping) algorithm is realized, and the 4DDW planning process structure diagram is shown in Figure 1.

*3.1. Horizontal Trajectory Planning.* Generally, multiple historical radar tracks exist in the overall space, and the use of HCDT enables accurate calculation and feature unification based on 2 main points. First, there are many types of historical trajectory data in the initial stage with low accuracy, and the error accumulation will occur with the increase of calculation volume, leading to distortion of calculation results. By introducing clustering optimization, the factors that lead to the accumulation of errors can be classified and screened to obtain the main influencing factors, then to provide support for subsequent accurate calculations. Second, due to the different flight speed and different flight path distances or ranges, the trajectory data on the time axis cannot be converged, which causes an atypical computational range. Through feature screening and HCDT model establishment, the initial phase data is placed in the same space. Considering the similarity problem of the initial phase data, the trajectory is considered as a time series to adjust, achieving consistency in track length.. Then, the comparison of the optimal warping is carried out, and the distance defect is avoided.

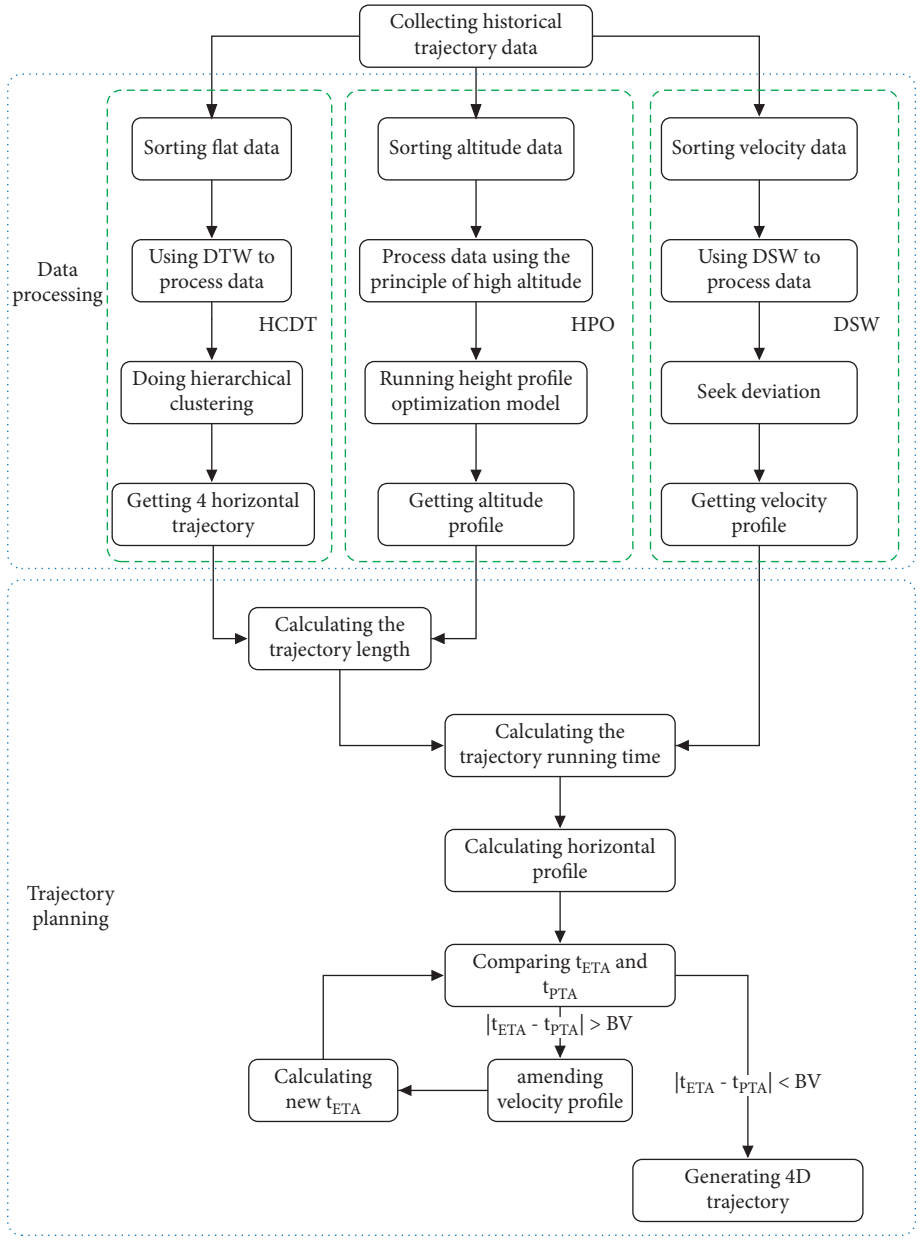


Figure 1: DDW planning process.

Assuming that flight path 1 is $X$ and flight path 2 is $Y$, there are

$$W = w_1, w_2, w_3, \ldots, w_k, \tag{1}$$

where $w_k = (i, j)$, the smaller the data, the higher the similarity of the flight path, and $i$ and $j$ are the similarities of the k-th flight path.

If there are adjacent flight path lengths $|X|$ and $|Y|$, there are

$$\max(|X|, |Y|) \le k \le |X| + |Y|. \tag{2}$$

Among them, K is the stretched length of adjacent sequences, as shown in Figure 2.

In order to ensure that the adjacent flight paths 1 and 2 are not repeated in the spatial data, the warping path must start from $w_1 = (1, 1)$ to $w_k = (|X|, |Y|)$ and meet the monotonic increase of $i$ and $j$ in the path $w_k = (i, j)$; then,

$$w_k = (i, j), w_{k+1} = (i', j'), \quad i \le i' \le i + 1, j \le j' \le j + 1. \tag{3}$$

If $w_n = (i, j)$ and $n = k$ already exist in the path, according to the basic principle of warping path, one of the three equations $(i + 1, j)$, $(i, j + 1)$, and $(I + 1, j + 1)$ must be selected for calculation in the next stage. Then, the warping distance matrix $D(i, j)$ is

$$\begin{aligned} D(i, j) = \text{Dist}(i, j) + \min\{&D(i - 1, j), \\ &D(i, j - 1), D(i - 1, j - 1)\}. \end{aligned} \tag{4}$$

Among them, Dist $(i, j)$ represents the distance between $i$ and $j$ in adjacent flight paths. $D(i, j)$ represents the similarity

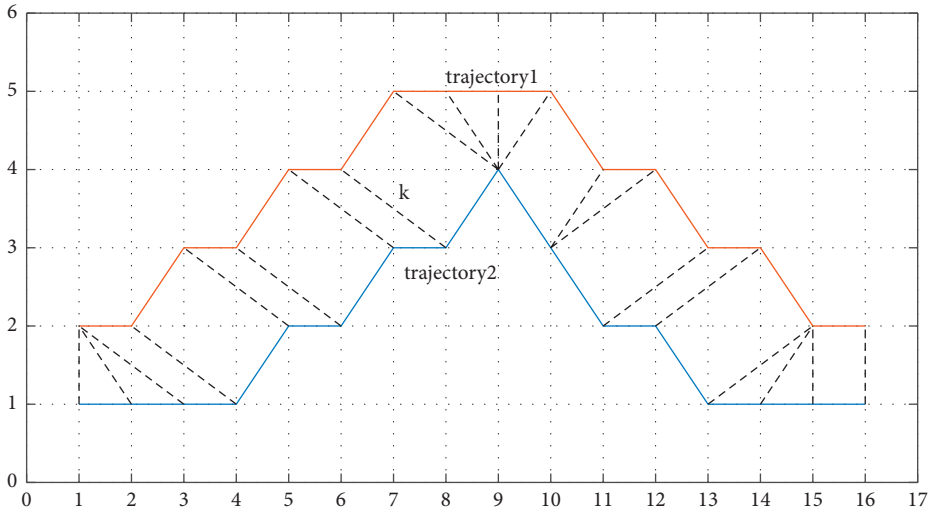


Figure 2: Dynamic time warping.

measurement value, which is used to process each point of flight path 1 before $i$ and each point of flight path 2 before $j$.

The warping path distance $D$ ($|X|$, $|Y|$) can be obtained via the former model. The smaller the $D$, the higher the similarity of the adjacent flight paths. The processing of flight trajectory accuracy and feature screening can be completed in the horizontal direction.

*3.2. Design of Nominal Velocity Profile.* During the design of the velocity profile model, all aircraft types and flight performance on the flight path in the approach phase are considered. DSW and multiple historical radar trajectories are used to establish the velocity profile model P, and the formula is as follows:

$$P = \{p_1, p_2, \ldots, p_n\}. \tag{5}$$

Among them, $p_i$ is the velocity profile of the i-th aircraft in flight. The average velocity profile is obtained by collating the $P$ set, namely, the nominal velocity profile $P_{STA}$, which represents the mean value in the data set and satisfies the nominal velocity profile $P_{STA} \in P$; then,

$$\sum_{i=1}^{n} \mathrm{DSW}(p_i, p_{sta}) \leq \sum_{i=1}^{n} \mathrm{DSW}(p_i, p_j). \tag{6}$$

Among them, DSW ($p_i$, $p_j$) is the dynamic spatial distance, and $j$ can be any value.

In order to improve the accuracy and reliability of the aircraft's nominal velocity profile, it is required that the collected data have the same length in time series. Through the comparison of sequence similarity, the consistency of data length can be improved by increasing the sampling times, so as to enable the effective comparison of time series with different lengths.

Suppose the two velocity profiles are

$$\begin{aligned} V^1 &= \left[v_1^1, v_2^1, \ldots, v_m^1\right], \\ V^2 &= \left[v_1^2, v_2^2, \ldots, v_n^2\right]. \end{aligned} \tag{7}$$

Set A as the velocity profile matrix for data comparison; then,

$$\begin{pmatrix} a_{11} & a_{12} & a_{13} & \ldots & a_{1n} \\ a_{21} & a_{22} & a_{23} & \ldots & a_{2n} \\ a_{31} & a_{32} & a_{33} & \ldots & a_{3n} \\ \ldots & \ldots & \ldots & a_{ij} & \ldots \\ a_{m1} & a_{m2} & a_{m3} & \ldots & a_{mn} \end{pmatrix}. \tag{8}$$

Among them, ($i$, $j$) are the velocities v1i and v2j on the profile, and $a_{ij}$ represents the distance between the two velocities. The curved path can be obtained by calculating the adjacent velocity profile and represented by $W = (w_1, w_2, \ldots w_k)$. The curved path is required to meet the continuity, monotonicity, and boundary conditions; then,

$$\left.\begin{aligned} &w_{k-1} = a_{i'j'}, w_k = a_{ij}, i - i' \leq 1, j - j' \leq 1 \\ &w_{k-1} = a_{i'j'}, w_k = a_{ij}, i - i' \geq 0, j - j' \geq 0 \\ &w_1 = a_{11}, w_k = a_{ij} \end{aligned}\right\}. \tag{9}$$

The DSW algorithm is conservative in limit path analysis, which is suitable for application in flight safety design. By setting the minimum total distance between speed $v^1$ and speed $v^2$, combined with the velocity profile matrix, there is

$$D(i, j) = a_{(i,j)} + \min\{D(i-1, j), D(i, j-1), D(i-1, j-1)\}, \tag{10}$$

where $a_{ij}$ is the natural length between two points $i$ and $j$ and the DSW distance between two adjacent velocity profiles is

$$\mathrm{DSW}\left(v^1, v^2\right) = \min\left(\sum_{i=1}^{k} w_i\right). \tag{11}$$

In order to further improve the validity of the calculation results, it is necessary to use the velocity profiles in sequence to calculate the DSW distance and introduce the concept of BV. It can enable the deviation value processing of each velocity profile with a more conservative way. The nominal velocity profile is formed by the velocity profile with the minimum deviation value, and the formula is as follows:

$$x_i = \sqrt{\frac{\left(\mathrm{DSW}^2\left(v^i, v^1\right) + \mathrm{DSW}^2\left(v^i, v^2\right) + \cdots + \mathrm{DSW}^2\left(v^i, v^n\right)\right)}{n}} + \mathrm{BV}. \tag{12}$$

*3.3. Altitude Profile Design.* In the instrument approach phase of flight procedures in the airport terminal area, CDO (continuous descent operation) is being promoted by ICAO as a new operation. CDO comprehensively considers the impact of level flight segment and the shortest descent segment on increasing airspace utilization, which can effectively improve the operating standards and enhance the safety guarantee in the landing phase. Therefore, the concept of CDO is adopted and designed for the altitude profile model. According to the features of the shortest distance projected to the ground during the descent phase of the CDO, an HPO model is established:

$$D = \min \sum_{n=1}^{n} D_n. \tag{13}$$

According to the constraint characteristics of the altitude of each descent phase on the critical obstacle, the constraint condition function is established:

$$H_{\mathrm{on}} \geq A_n + \mathrm{MOC}_n. \tag{14}$$

Since the landing phase of an aircraft is divided into multiple approach phases, and the optimal descent gradient requirements for each approach phase are different, the descent gradient limiting function is established:

$$\frac{H_i - H_{i-1}}{D_{(i\sim i-1)}} = \mathrm{Gr}_i. \tag{15}$$

Considering the comfort requirements of civil passenger aircraft, add the constraint of decline rate:

$$\frac{H_i - H_{i-1}}{T} = \mathrm{ROD}. \tag{16}$$

If the optimal descent gradient is taken for this segment and there are no critical obstacles, then,

$$D_i = D_{(i\sim i-1)} = \frac{\left(H_i - H_{i-1}\right)}{\mathrm{Gr}_i}. \tag{17}$$

If there are critical obstacles in this segment, no gradient optimization will be implemented.

From Formulas (12)–(16), $D_i$ represents the projection distance of the i-th segment on the ground, $H_{\mathrm{on}}$ represents the flight height of the $n$-th obstacle on the segment, $A_n$ represents the altitude of the $n$-th obstacle, $\mathrm{MOC}_n$ represents the $n$-th obstacle MOC (Minimum Obstacle Clearance) where the obstacle is located, $i$ represents the waypoint or fix, $D_{(i\sim i-1)}$ represents the distance from the fix $i$ to the $i-1$, $\mathrm{Gr}_i$ represents the optimal descent gradient of segment $i$, $T$ is the time required to establish the height for the decrease, and the ROD is the decrease rate.

By preprocessing and feature classification of historical trajectory data, using HCDT, DSW, and HPO for model establishment and calculation, then multiple initial horizontal trajectories, altitude profiles, and velocity profiles can be obtained. This can provide basic parameters for flight trajectory generation.

## 4. Simulation Experiments

The simulation experiment is designed according to the 4D flight path dynamic warping model, as follows:

(1) Horizontal flight path experiment: the existing historical radar trajectory is used for dynamic time warping, and hierarchical clustering is carried out for the results after warping. The results obtained by using hierarchical clustering are combined with the instrument arrival route to derive the number of horizontal trajectory and operating parameters.

(2) Velocity profile experiment: the DSW is used to warp the velocity profile obtained from the existing historical radar track, and the velocity profile with the smallest deviation is calculated and selected as the nominal velocity profile.

(3) Altitude profile experiment: to analyze the existing historical radar data, sort the altitude range of the waypoints in the space, combine the horizontal trajectory parameters with the waypoint after sorting, and use the optimized model to complete the corresponding height profile design.

(4) Sort out the horizontal trajectory, velocity profile, and altitude profile information in the above simulation experiments, and calculate the complete 4D flight path.

*4.1. Horizontal Flight Path Design.* The track data of nearly 180 days during the approach phase of the airport are collected as samples, and Airbus 319 is used as the experimental aircraft to conduct time warping and track clustering for the existing historical radar track, and the schematic diagram of the existing historical radar track sample is established, as shown in Figure 3. HCDT (Formulas (1)–(4)) is used to normalize the existing historical radar track, and then hierarchical clustering is used to perform cluster analysis on the warping results. The specific results are shown in Figure 4.

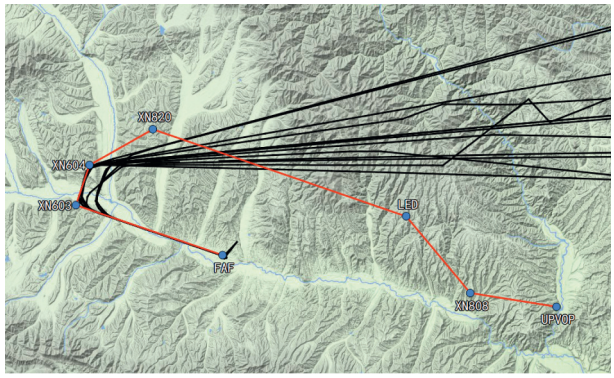


Figure 3: Historical radar trajectory.

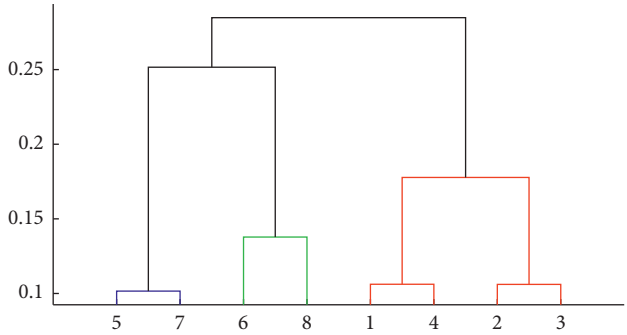


Figure 4: Historical trajectory clustering result map.

In order to make the calculation results more concentrated and representative, the minimum square of deviance is set as $2 \times 10^9$ to prune the trajectory clustering analysis. Each pruned tree can be regarded as a cluster, and 4 trajectory clustering results can be obtained, and the average value is used to determine the trajectory clustering. Based on similar results, compared with the flight procedures of the subject's airport approach phase, 4 horizontal approach route designs are finally obtained, as shown in Figure 5.

*4.2. Velocity Profile Design.* The same airport is selected as the experimental airport. The experimental aircraft is Airbus 319. The existing historical radar trajectories are collected, and the flight speed, spatial horizontal position, flight distance, and other information are screened to establish the original flight velocity profile, as shown in Figure 6.

Through the original velocity profile data, DSW (Formulas (5)–(10)) is used to calculate the DSW distance of each velocity profile. The results are shown in Table 1, where $v1$ to $v8$ represent eight velocity curves.

The DSW distance is obtained according to the derivation of the velocity profile, and the deviation value of the relevant velocity profile is calculated by Formula (11). The results are shown in Table 2. According to ICAO's suggestion for the construction of flight safety conflict value, BV should be introduced into the total system error to be treated conservatively. So the simulation experiment adopts ICAO's recommended value in the approach phase, and BV is 1 (NM) [34]. Collect the deviation values for analysis, and take the minimum deviation value to form the nominal velocity profile parameter according to the conservative principle [6]. Table 2 shows that the deviation of $v4$ is the smallest, then $v4$ is selected as the nominal velocity profile, and a schematic diagram of the nominal velocity profile established is as shown in Figure 7.

*4.3. Altitude Profile Design.* The same airport is selected as the experimental airport, and the historical radar tracks in the arrival phase are collected for analysis to obtain the altitude range of the approaching aircraft, as shown in Table 3. The diagram of the standard altitude profile is established by the principle of high altitude, as shown in Figure 8.

Obstacle data during arrival and approach phases are collected, as shown in Table 4.

In accordance with ICAO's recommendations for CDO, the original altitude profile is optimized by using HPO model (Formulas (12)–(15)). The obstacle climbing condition is analyzed through the data in Table 4, and the optimal descent gradient for the approach segment is set to 3% (<8%) [35]. The optimization results can be derived. The relevant data is shown in Table 5, where $A3$ is a new waypoint. The optimized altitude profile is shown in Figure 9.

Through the comparison between Figures 8 and 9, it can be found that, after the optimization implemented by using the HPO model, the horizontal flight segment distance is increased by 35.4 km, and the descending phase of descent gradient is within the flight standard safety value consistently. So, the HPO ensures flight safety and improves flight economy, meeting the constraints.

## 5. Result Analysis

According to the experimental design and calculation results of the horizontal trajectories, velocity profile, and altitude profile, the flight path optimization of the experimental airport from the arrival to the approach phase is completed. Finally, the flight time required by the optimized flight path is calculated and four typical optimization results are selected to form the distance and schedule, as shown in Table 6.

According to the optimization results, $t_{\mathrm{PTA}}$ (planned time of arrival) and $t_{\mathrm{ETA}}$ (estimated time of arrival) are compared and analyzed. The threshold is set as 5 seconds, which can not only guarantee the calculation efficiency of trajectory planning but also ensure the accuracy of trajectory planning. Combined with the analysis of the optimization results in Table 6, it is shown that the flight time of trajectory 4 is 966 s, which is the closest figure comparing to the planned time of arrival (960 s). The calculation difference between $t_{\mathrm{PTA}}$ and $t_{\mathrm{ETA}}$ is 6 seconds, which exceeds the preset threshold. Therefore, the nominal velocity profile shown in Figure 7 needs to be adjusted [5]. The corrected speed is shown in Table 7, and the corrected nominal velocity profile is shown in Figure 10.

The corrected nominal velocity profile and horizontal profile No. 4 are used for analysis. The flight time is calculated as 960.2 seconds, which is 0.2 seconds away from the

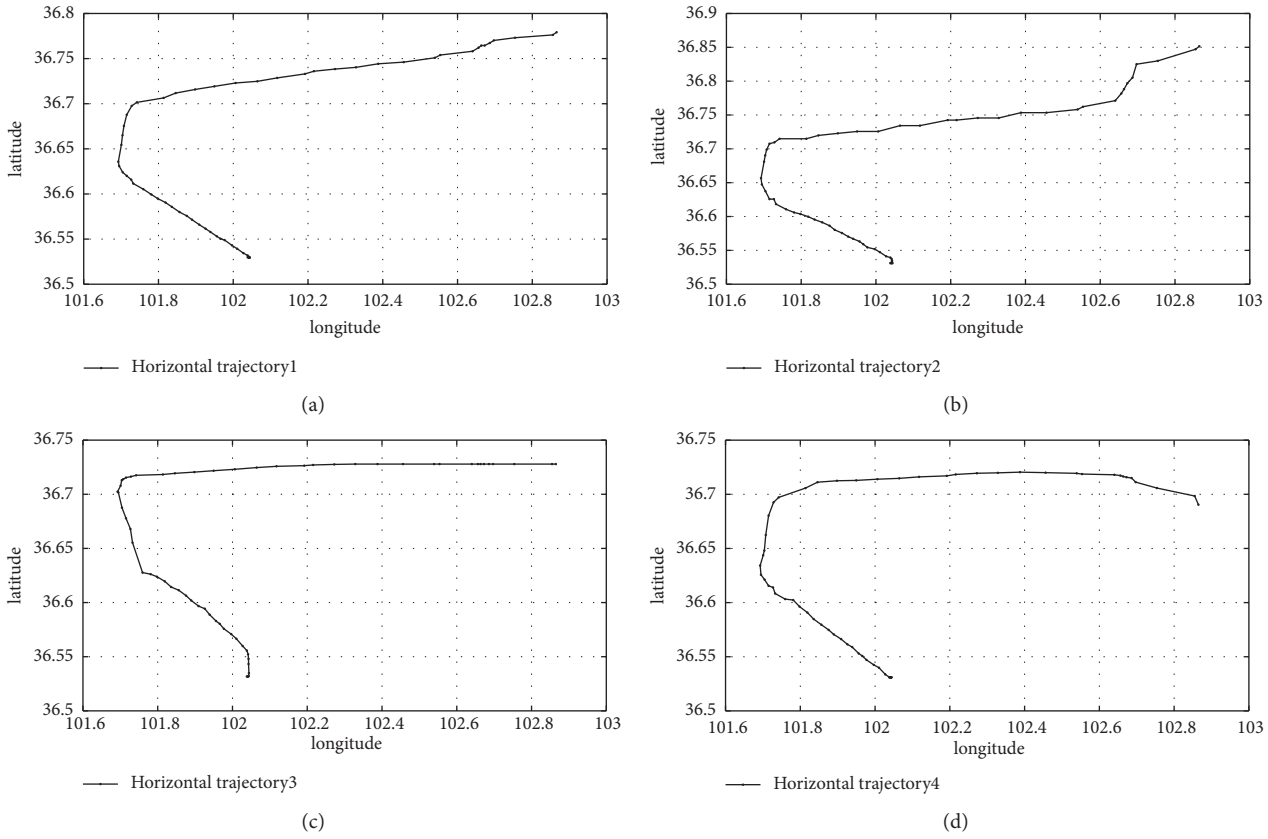


Figure 5: A1 approach horizontal trajectory.

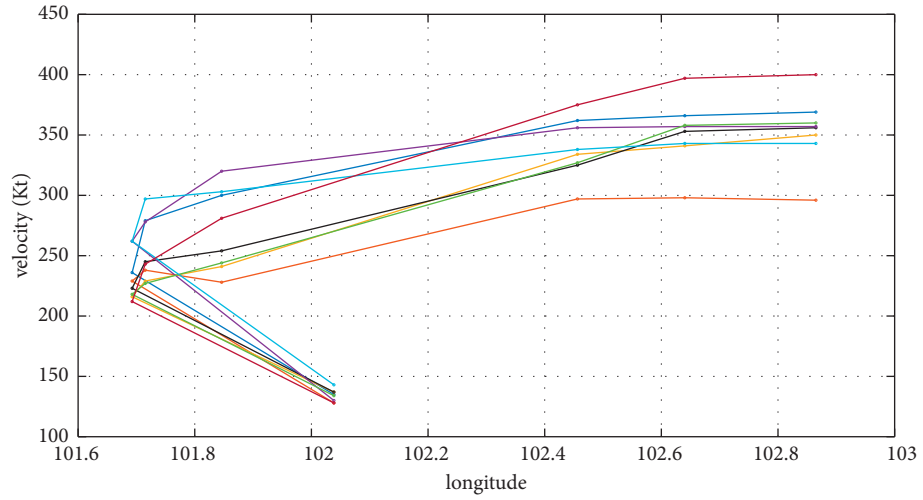


Figure 6: Schematic diagram of the original velocity profile.

960 seconds required by $t_{PTA}$, and does not exceed the preset threshold. Based on this result, the original flight path of the airport approach flight of the experimental object is generated, and the 4D flight path is optimized by using the 4DDW, as shown in Figure 11.

According to the comparison of simulation experiment results, it is found that the original flight path (right of Figure 11(b)) starts from $A1$ to $A8$, in which there is no $A3$ point, and the time dimension is not planned for the whole flight path. The 4D flight path (left of Figure 11(a)) starts from $A1$ to $A8$, $A3$ is a new point, and the descend phase starts at $A3$, and the level flight from $A1$ to $A3$ makes the 4D flight path much closer to the runway. When starting to descend at a higher altitude, the maneuverability and economy of the approaching aircrafts can be improved. In addition, 4D flight paths can effectively enhance efficiency of

Table 1: DSW distance.

| | $v1$ | $v2$ | $v3$ | $v4$ | $v5$ | $v6$ | $v7$ | $v8$ |
|---|---|---|---|---|---|---|---|---|
| $v1$ | 0 | 249 | 157 | 106 | 79 | 109 | 128 | 134 |
| $v2$ | 249 | 0 | 172 | 191 | 310 | 195 | 243 | 333 |
| $v3$ | 157 | 172 | 0 | 57 | 166 | 44 | 184 | 213 |
| $v4$ | 106 | 191 | 57 | 0 | 97 | 34 | 156 | 184 |
| $v5$ | 79 | 310 | 166 | 97 | 0 | 130 | 95 | 215 |
| $v6$ | 109 | 195 | 44 | 34 | 130 | 0 | 203 | 168 |
| $v7$ | 128 | 243 | 184 | 156 | 95 | 203 | 0 | 270 |
| $v8$ | 134 | 333 | 213 | 184 | 215 | 168 | 270 | 0 |

Table 2: Deviation.

| $v1$ | $v2$ | $v3$ | $v4$ | $v5$ | $v6$ | $v7$ | $v8$ |
|---|---|---|---|---|---|---|---|
| 138.1 | 233.4 | 145.1 | 123.3 | 163.6 | 133 | 180 | 211.7 |

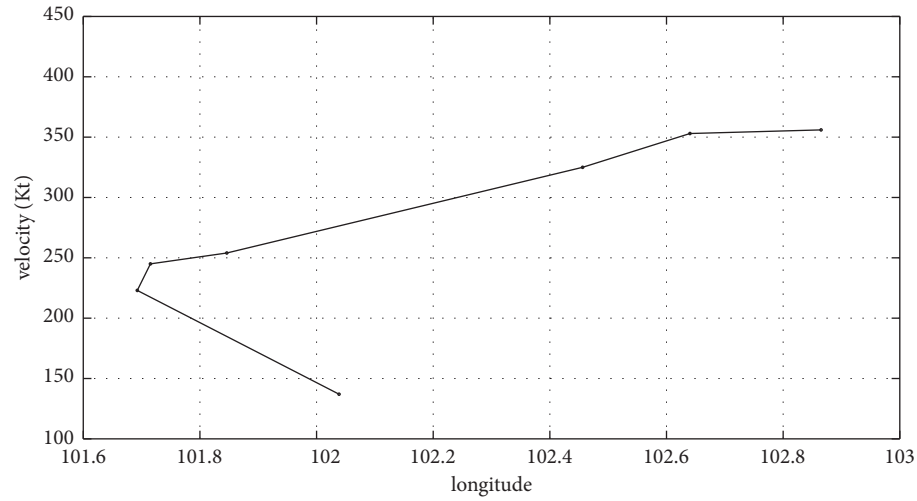


Figure 7: Nominal velocity profile.

Table 3: Altitude range of each waypoint.

| Waypoint | $H$(ft) |
|---|---|
| $A1$ | 17674–19426 |
| $A2$ | 17674–18825 |
| $A4$ | 17100–17726 |
| $A5$ | 12749–13901 |
| $A6$ (IAF) | 12149–12776 |
| $A7$ (IF) | 11152–11949 |
| $A8$ (FAF) | 6373–6883 |

flight sequencing, improve flight safety, and reduce conflicts and congestion in the terminal area when planning with a time dimension.

## 6. Advancement Description

At present, the similarity research mainly focuses on the construction of 4D flight path, and there are different consideration for the convenience and integrity of the algorithm. Among them, the four-dimensional trajectory planning algorithm, based on planned arrival times, is more commonly used [36]. According to Table 3 and the original flight data, the simulation experiment is established, and the typical algorithm is used to generate the 4D flight path. The calculation results are shown in Figure 12. The solid line is the calculation result of typical algorithm, and the dotted line is the calculation result of 4DDW.

Compared with the calculation results, it is found that, in terms of flight attitude, 4DDW has level flight and descent phase. It can reasonably handle the relationship between safety and economy of obstacle climbing. In terms of flight path structure, 4DDW has the characteristics of continuous descent, not only optimizing operating standards, but also ensuring the rate of normal flights. In terms of spatial path range, 4DDW demonstrates the characteristics of spatial range convergence, which provides basic conditions for increasing airspace capacity.

There are two reasons for the differences in calculation results. First, because the 4DDW algorithm is constructed by three profiles, time dimension planning is also considered, and threshold presets and comparisons are used. So, the calculation results reflect the optimization of flight time and flight distance. Second, because the 4DDW altitude profile

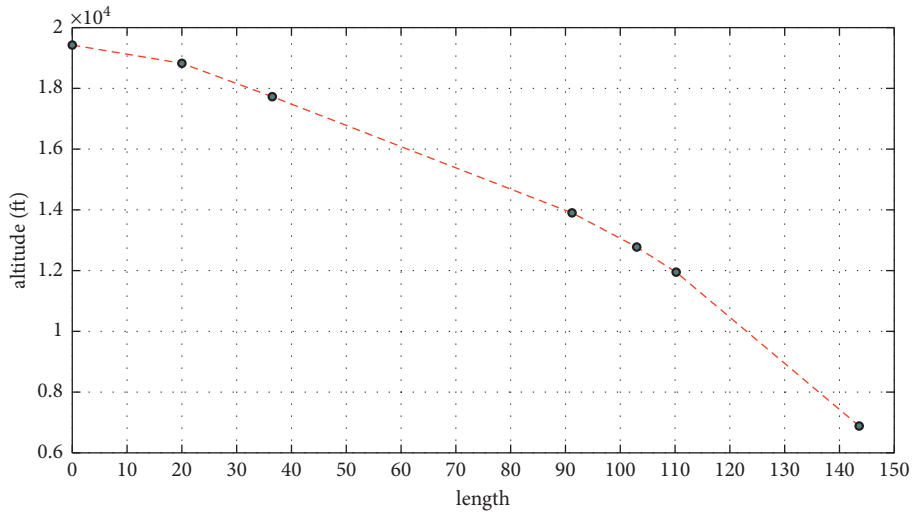


Figure 8: Schematic diagram of height profile.

Table 4: Observer data.

| Serial number | Magnetic bearing (°) | Distance (km) | Altitude (ft) | Affected flight procedures and take-off path area |
|---|---|---|---|---|
| 1 | 092 | 38.722 | 9675 | RWY29/initial approach |
| 2 | 125 | 29.240 | 8802 | RWY29/intermediate approach |

Table 5: The altitude of each anchor point and the distance from point A1.

| Serial number | Waypoint | Altitude (ft) | Distance from point *A*1 (km) |
|---|---|---|---|
| 1 | *A*1 | 19426 | 0 |
| 2 | *A*2 | 19426 | 20 |
| 3 | *A*3 | 19426 | 35.4 |
| 4 | *A*4 | 19319 | 36.5 |
| 5 | *A*5 | 13937 | 91.2 |
| 6 | *A*6 (IAF) | 12776 | 103 |
| 7 | *A*7 (IF) | 11949 | 110.2 |
| 8 | *A*8 (FAF) | 6883 | 143.6 |

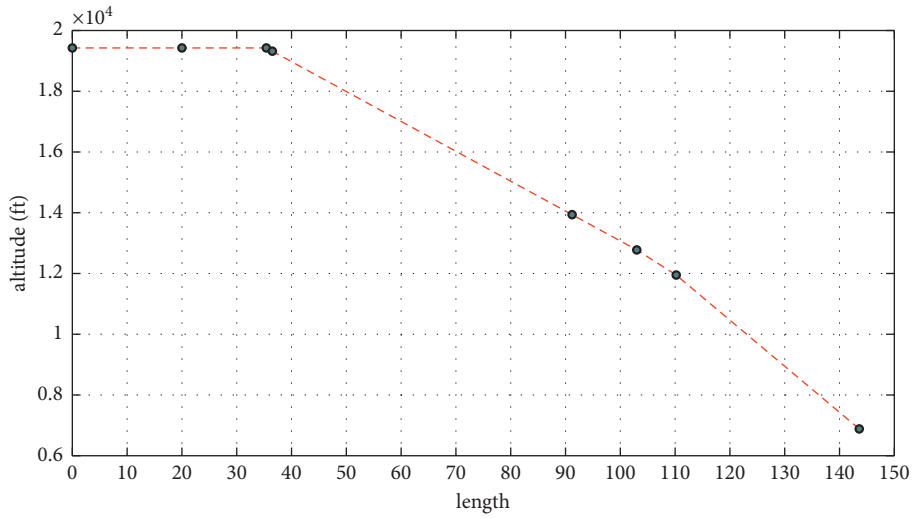


Figure 9: Schematic diagram of optimized height profile.

Table 6: Typical flight trajectory and required running time.

| Trajectory | Trajectory length (km) | Running time (s) |
|---|---|---|
| 1 | 141.4 | 950 |
| 2 | 145.0 | 973 |
| 3 | 141.7 | 953 |
| 4 | 143.6 | 966 |

Table 7: Corrected speed.

| Waypoint | *A*1 | *A*2 | *A*4 | *A*5 | *A*6 (IAF) | *A*7 (IF) | *A*8 (FAF) |
|---|---|---|---|---|---|---|---|
| Corrected speed (kt) | 360 | 357 | 326 | 255 | 248 | 224 | 137 |

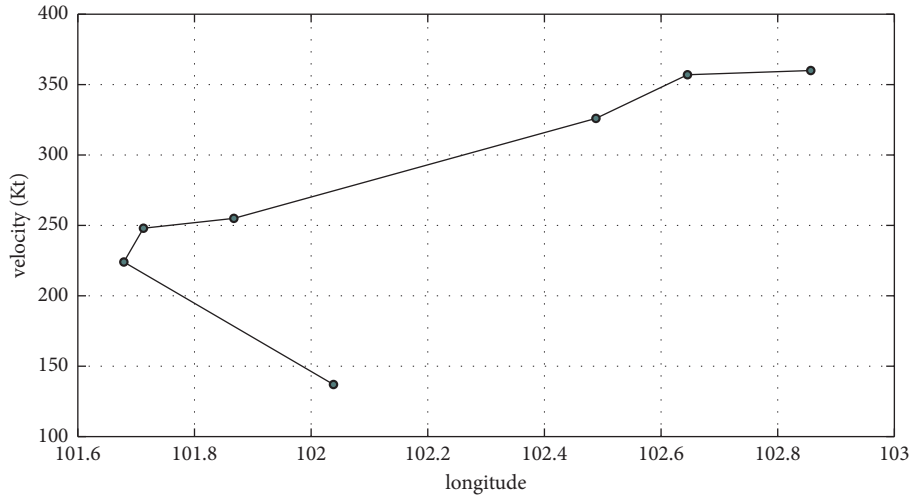


Figure 10: Corrected nominal velocity profile.

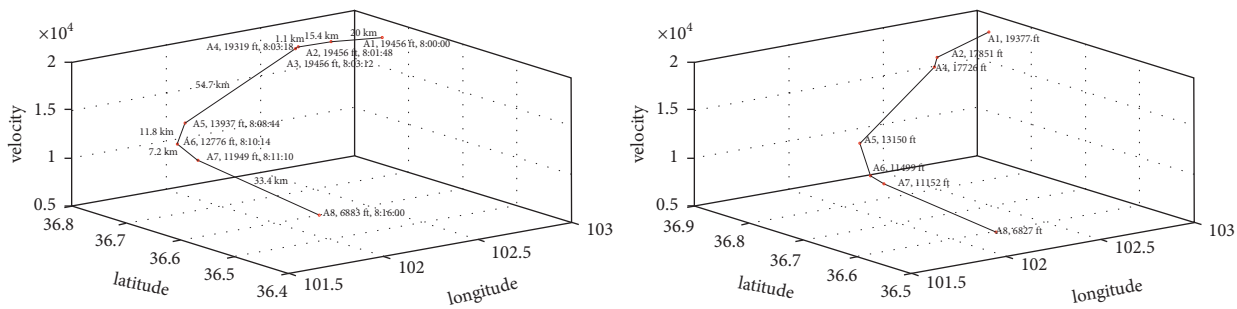


Figure 11: (a) 4D flight path planning diagram and (b) original flight path diagram.

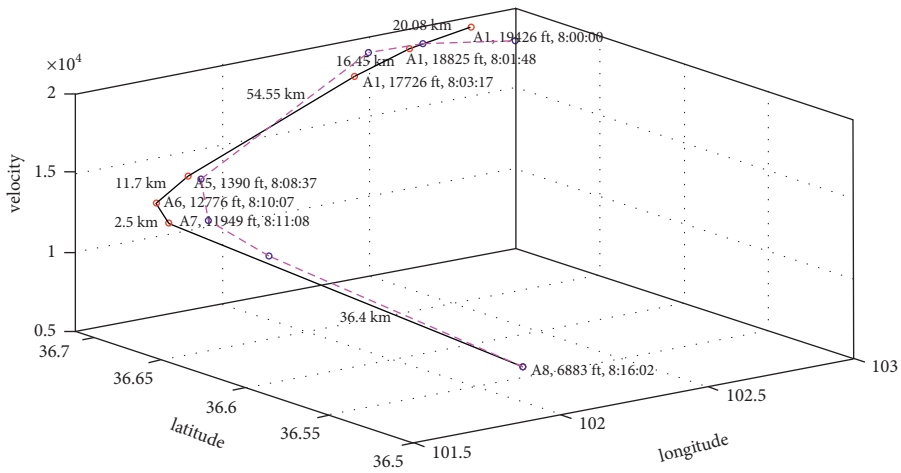


Figure 12: Comparison chart of flight path calculation results between typical algorithm and 4DDW.

introduces the concept of CDO, and the level flight, descent, and obstacle climbing analysis are included in the 4D flight path calculation, it can optimize the operational standards and the convergence space range. 4DDW fully reflects the comprehensiveness and rationality in dealing with problems such as flight path prediction and is advanced compared with current common algorithms.

## 7. Conclusions

By analyzing the results of simulation experiments and experimental calculations comparison, we have the following conclusions:

(1) With multidimensional model, 4DDW sorts out the data characteristics of each flight phase, which make calculation results in accordance with the data classification and enrich the data types and features required for flight environment measurement.

(2) 4DDW relies on the design of buffer and threshold values to make the aircraft spatial waypoint planning conform to ICAO's flight standard recommendations and provides an accurate planning method for each point for wide-range spatial path identification. Also the basis for similarity judgment is set and the probability of position overlap is reduced.

As a foundation, 4DDW can be provided for verifying the current flight procedures in the aspect of science, rationality, and economy. It can also optimize the flight procedures in the airport terminal area to ensure flight safety.

## Abbreviations

HCDT: Hierarchical clustering dynamic time warping
DSW: Dynamic spatial warping
HPO: Height profile optimization
4DDW: 4D dynamic warping
$t_{PTA}$: Planned time of arrival
$t_{ETA}$: Estimated time of arrival
V: Velocity
BV: Buffer value
CDO: Continuous descent operations
4D: Four-dimensional
ICAO: International Civil Aviation Organization
ASBU: Aviation System Block Upgrade
DTW: Dynamic time warping.

## Data Availability

The data used to support the findings of this study are included within the article.

## Disclosure

The funders had no role in the design of the study, in the collection, analyses, or interpretation of data, in the writing of the manuscript, or in the decision to publish the results.

## Conflicts of Interest

The authors declare that there are no conflicts of interest.

## Authors' Contributions

X. Li and H. Yan conceptualized the study and developed methodology. Y. Zhang provided software and visualized the study. X. Li, H. Yan, and Y. Zhang contributed to the validation and funding acquisition. H. Yan prepared the original draft. X. Li contributed to project administration and reviewed and edited the manuscript. All authors have read and agreed to the published version of the manuscript.

## Acknowledgments

This research was funded by Educational Talents Program of Civil Aviation Administration of China, Grant no. 14002600100019J104, and scientific research project of Civil Aviation Flight University of China, Grant nos. 2019-53 and XM2414.

## References


[1] L. G. Zhou, X. M. Tang, and M. Tang, "4D trajectory prediction of aircraft taxiing based on fitting velocity profile," *Aeronautical Computing Technique*, vol. 45, no. 01, pp. 35–39+44, 2015.

[2] B. Zheng, H. Gao, X. Ma, and X. Zhang, "Graph partition based on dimensionless similarity and its application to fault diagnosis," *IEEE Access*, vol. 9, pp. 35573–35583, 2021.

[3] N. Mishra, H. K. Soni, H. K. Soni, S. Sharma, and A. K. Upadhyay, "Development and analysis of artificial neural network models for rainfall prediction by using time-series data," *International Journal of Intelligent Systems and Applications*, vol. 10, no. 1, pp. 16–23, 2018.

[4] Y. Li, Y. Chen, J. Zhong, and Z. Huang, "Niching particle swarm optimization with equilibrium factor for multi-modal optimization," *Information Sciences*, vol. 494, pp. 233–246, 2019.

[5] R. Zeng and Y. Wang, "A chaotic simulated annealing and particle swarm improved artificial immune algorithm for flexible job shop scheduling problem," *EURASIP Journal on Wireless Communications and Networking*, vol. 2018, no. 1, pp. 101–123, Article ID 101, 2018.

[6] K. R. Kalidindi, P. S. V. Gottumukkala, and R. Davuluri, "Derivative-based band clustering and multi-agent PSO optimization for optimal band selection of hyper-spectral images," *The Journal of Supercomputing*, vol. 76, no. 1, pp. 5873–5898, 2020.

[7] X. Ma, X. X. Zhang, H. W. Wang, S. Ding, and X. Li, "An operational safety evaluation method for manned transport aircraft and large UAV in mixed airspace," *Mathematical Problems in Engineering*, vol. 2021, Article ID 6636794, 12 pages, 2021.

[8] H. Li, A. P. Teixeira, and C. Guedes Soares, "A two-stage Failure Mode and Effect Analysis of offshore wind turbines," *Renewable Energy*, vol. 162, pp. 1438–1461, 2020.

[9] X. Zhang, M. Fan, D. Wang, P. Zhou, and D. Tao, "Top-k feature selection framework using robust 0-1 integer programming," *IEEE Transactions on Neural Networks and Learning Systems*, vol. 32, no. 7, pp. 3005–3019, 2021.

[10] J. Hu, H. Chen, A. A. Heidari et al., "Orthogonal learning covariance matrix for defects of grey wolf optimizer: insights, balance, diversity, and feature selection," *Knowledge-Based Systems*, vol. 213, Article ID 106684, 2020.

[11] J. Marion, P. Letortu, and T. Claire, "UAV survey of a coastal cliff face-Selection of the best imaging angle," *Measurement*, vol. 24, pp. 110–117, 2019.

[12] D. Zhao, L. Liu, F. Yu et al., "Chaotic random spare ant colony optimization for multi-threshold image segmentation of 2D Kapur entropy," *Knowledge-Based Systems*, vol. 216, Article ID 106510, 2020.

[13] R. U. Khan, X. Zhang, R. Kumar, A. Sharif, N. A. Golilarz, and M. Alazab, "An adaptive multi-layer botnet detection technique using machine learning classifiers," *Applied Sciences*, vol. 9, no. 11, p. 2375, 2019.

[14] N. A. Golilarz, M. Mirmozaffari, T. A. Gashteroodkhani et al., "Optimized wavelet-based satellite image de-noising with multi-population differential evolution-assisted Harris hawks optimization algorithm," *IEEE Access*, vol. 8, pp. 133076–133085, 2020.

[15] H. Li and C. G. Soares, "Reliability analysis of floating offshore wind turbines support structure using hierarchical Bayesian network," in *Proceedings of the 29th European Safety and Reliability Conference*, pp. 2489–2495, Research Publishing Services, cop., Hanover, Germany, 22 September 2019.

[16] J. Liu, J. F. Zhang, H. B. Zhu, and G. H. Ma, "Four-dimension trajectory planning based on scheduled time of arrival," *Aeronautical Computing Technique*, vol. 41, no. 07, pp. 325–338, 2016.

[17] C. Wang, X. H. Xu, and F. Wang, "ATC serviceability analysis of terminal arrival procedures using trajectory clustering," *Journal of Nanjing University of A eronautics & A stronautics*, vol. 45, no. 01, pp. 130–139, 2013.

[18] G. H. Ma, J. F. Zhang, F. Wang, and Q. Cheng, "A 4D trajectory planning method based on historical radar tracks of air traffic," *Traffic information and safety*, vol. 33, no. 04, pp. 106–112, 2015.

[19] S. Ding, J. Guan, and J. Liu, "4D flight trajectory prediction and conflict warning in terminal area," *Science Technology and Engineering*, vol. 21, no. 28, pp. 12307–12313, 2021.

[20] L. H. Zhang, Z. Y. Feng, Q. Cheng et al., "Fast query-by-example spoken term detection algorithm based on dynamic time warping," *Application Research of Computers*, vol. 31, no. 06, pp. 1688–1692, 2014.

[21] G. Mantena, S. Achanta, and K. Prahallad, "Query-by-example spoken term detection using frequency domain linear prediction and non-segmental dynamic time warping," *IEEE/ACM Transactions on Audio, Speech, and Language Processing*, vol. 22, no. 5, pp. 946–955, 2014.

[22] B. Khorram and M. Yazdi, "A new optimized thresholding method using ant colony algorithm for MR brain image segmentation," *Journal of Digital Imaging*, vol. 32, no. 1, pp. 162–174, 2019.

[23] General Aviation Branch of China Air Transport Association, *China's Development Report on Civil Drones 2019*, pp. 303–320, 2020.

[24] M. Mavrovouniotis and S. Yang, "Training neural networks with ant colony optimization algorithms for pattern classification," *Soft Computing*, vol. 19, no. 6, pp. 1511–1522, 2015.

[25] N. A. Golilarz, H. Demirel, and H. Gao, "Adaptive generalized Gaussian distribution oriented thresholding function for image de-noising," *Int. Jou. Adv. Com. Sci. App*, vol. 10, pp. 10–15, 2019.

[26] W. Schmidt and P. Groche, "Wear prediction for oscillating gear forming processes using numerical methods," *Key Engineering Materials*, vol. 767, pp. 283–289, 2018.

[27] ZH. Zhang, F. Min, GS. Chen, and S. P. Shen, "Tri-partition state alphabet-based sequential pattern for multivariate time series," *Cogn Comput.*, 2021.

[28] Wu Deng, X. Zhang, Y. Zhou et al., "An enhanced fast non-dominated solution sorting genetic algorithm for multi-objective problems," *Information Sciences*, vol. 585, pp. 441–453, 2022.

[29] H. Cui, Y. Guan, H. Chen, and W. Deng, "A novel advancing signal processing method based on coupled multi-stable stochastic resonance for fault detection," *Applied Sciences*, vol. 11, no. 12, p. 5385, 2021.

[30] H. Chen, A. A. Heidari, H. Chen, M. Wang, Z. Pan, and A. H. Gandomi, "Multi-population differential evolution-assisted Harris hawks optimization: framework and case studies," *Future Generation Computer Systems*, vol. 111, pp. 175–198, 2020.

[31] M. Yazdi, A. Nedjati, E. Zarei, and R. Abbassi, "A novel extension of DEMATEL approach for probabilistic safety analysis in process systems," *Safety Science*, vol. 121, pp. 119–136, 2020.

[32] C. Yu, M. Chen, and K. Cheng, "SGOA: annealing-behaved grasshopper optimizer for global tasks," *Engineering with Computers*, pp. 1–28, 2021.

[33] B. Zheng and X. Ma, "Application of improved Kohonen network in aeroengine classification fault diagnosis," *Aeroengine*, vol. 46, no. 2, pp. 23–29, 2020.

[34] C.-G. Huang, H.-Z. Huang, and Y.-F. Li, "A bidirectional LSTM prognostics method under multiple operational conditions," *IEEE Transactions on Industrial Electronics*, vol. 66, no. 11, pp. 8792–8802, 2019.

[35] K. Shailaja and B. Anuradha, "Improved face recognition using a modified PSO based self-weighted linear collaborative discriminant regression classification," *Journal of Engineering and Applied Sciences*, vol. 12, no. 23, pp. 7234–7241, 2017.

[36] X. Ma, X. Huang, L. Lu, and X. Li, "A design method of UAV flight protection area based on the statistical analysis of flight path deviation," *IOP Conference Series: Materials Science and Engineering*, vol. 1043, no. 4, 2021.